Reaction Kinetics, Mechanisms and Catalysis (2024) 137:1337–1353
https://doi.org/10.1007/s11144-024-02596-z

Kinetic analysis of alumina leaching from calcined Owhe kaolinite in HNO_3 and H_2O_2 solution

Ikechukwu Abuchi Nnanwube[1] · Mabel Keke[2] · Okechukwu Dominic Onukwuli[1,3]

Received: 29 November 2023 / Accepted: 16 February 2024 / Published online: 5 April 2024
© Akadémiai Kiadó, Budapest, Hungary 2024

Abstract

In this work, the feasibility of nitric acid (HNO_3) and hydrogen peroxide (H_2O_2) binary solution as a leachant for alumina leaching from Owhe kaolinite was examined. The leaching was carried out by batch process. Least squares method was deployed to examine the experimental results. The results show that the percentage of alumina dissolved recorded an increase with increase in the concentration of H_2O_2 and temperature and recorded a reduction with increase in solid/liquid (S/L) ratio and particle size. Chemical reaction was established as the rate-determining step. About 89% alumina was leached on the average with activation energy (E_a) of 4.406 kJ/mol while the overall rate constant was 1.067 s^{-1}. A binary solution of HNO_3 and H_2O_2 showed viability for Owhe kaolinite leaching. Analysis of residue remaining after leaching by energy dispersive spectrometer (EDS) showed the major elements found in the residues as silicon, aluminum, and titanium.

Keywords Kaolinite · Kinetics · Leaching · Alumina · Nitric acid

Introduction

Kaolinite is composed of aluminum and silicon ($Si_2Al_2O_5(OH)_4$) and its reduction would result in an aluminum/silicon alloy. The recovery of alumina from kaolinite either in pilot or industrial scale has been explored by various researchers using various means. This is due to the numerous technological and industrial uses of alumina. Various meta-stable states of alumina exist, among which are γ-, β, and α-alumina.

✉ Ikechukwu Abuchi Nnanwube
ik.nnanwube@gmail.com

[1] Chemical Engineering Department, Madonna University, Akpugo, Nigeria

[2] Chemical Engineering Department, Delta State University of Science and Technology, Ozoro, Nigeria

[3] Chemical Engineering Department, Nnamdi Azikiwe University, Awka, Nigeria

Among these states, γ-alumina has been identified as the most widely utilized, having found application in abrasive and thermal wear coatings, structural composites for spacecraft, automotive and petroleum industries as a catalyst and catalyst substrates. Some recently reported studies revealed that γ-alumina is stable thermodynamically when compared to α-alumina especially on attainment of a critical surface area [1, 2]. In addition, the sintering behavior of alumina and silicon carbide fibers can be promoted by nano γ-alumina powder. These and other uses such as its ability to improve the electrical properties of insulators and other polymeric insulating materials make its production and study extremely important [1, 2].

The Bayer's procedure which utilizes an acidic mineral known as bauxite as its natural resource is the main route from which aluminum and its compounds are manufactured via alkaline leaching. Globally, the Bayer process accounts for more than 90% of alumina production, with bauxite residue forming a great percentage of the by-products of the extraction process. The Bayer bauxite residue contain a lot of alkaline materials such as $NaAlO_2$, NaOH, Na_2CO_3, $NaSiO_3$, zeolite sodium alumino-silicate hydrate, among others. These waste products are usually costly and difficult to deal with and can also pollute the environment [3].

Calcinations temperature and calcinations time have been found to have a considerable effect on the yield of alumina in the chemical procedures for alumina extraction from clay [3]. To maximize the degree of alumina extraction from clay, the influence of factors such as the concentration of the lixiviant, clay particle size, stirring rate, leaching temperature, calcinations temperature, and solid/liquid ratio have been worked on by various researchers [3–5]. However, no study has been reported—to our knowledge—on the use of a binary solution of HNO_3 and H_2O_2 for alumina leaching from Owhe kaolinite despite the high alumina content of the clay. Both HNO_3 and H_2O_2 have been widely applied in leaching operations due to their oxidative properties [4–8].

Hence, this study was aimed at exploring the effectiveness of HNO_3 and H_2O_2 binary solution for the leaching of alumina from Owhe kaolinite via kinetics studies. In addition, previous studies made use of the shrinking core models in analyzing the experimental data. No study—known to the authors—have been carried out on the use of least squares method in the analysis of alumina leaching from kaolinite. This method was also explored in this study. Least squares method helps to assess whether the theoretical function gives a rational description of the measured data. This research has also re-echoed the necessity of finding an alternative means of alumina production, especially from kaolinitic clay as a replacement to bauxite which is not found in large quantity in Nigeria and decreasing in quantity and quality on the global scale.

Materials and methods

Materials and preparation of sample

The kaolinite utilized in this work was collected from Owhe in Isoko North L.G.A. of Delta State, Nigeria. Muffle furnace was used to calcine the kaolinite in the

temperature range of 500–800 °C for 1 h to enhance the leaching process after drying it in the sun for 3 days. The calcined clay was sieved to obtain different size fractions: < 75, 75–106, 106–250, 250–350, and < 408 µm, using ASTM sieves. All experiments were executed with the < 75 µm fraction except when stated otherwise. Reagents of analytical grade were used for the study. The chemical composition examination of the raw clay was carried out by energy dispersive X-ray fluorescence spectroscopy (EDXRF) (Quant'X model). Morphology and phase analysis of the clay were performed with scanning electron microscope (SEM) (Phenom Pro X SEM analyzer) and X-ray diffractometer (XRD) (Rigaku miniflex 6000 model) [4].

Leaching procedure

Experiments were conducted with the calcined samples of the clay to obtain the best calcinations temperature. The experiments were performed for 2.5 h in a 500 mL Pyrex glass reactor placed on a temperature-regulated hot plate fitted with a stirrer. The reactor was connected to a condenser to prevent evaporation. 2 g of the calcined kaolinite was added to 100 mL of the binary solutions. The temperature was adjusted to the preferred value while stirring was maintained at 500 rpm in a time range of (20–150 min). The range of the process variables used for the kinetic study include acid concentration of (2–12 M), reaction temperature of (40–90 °C), S/L ratio of (0.015–0.043 g/mL) and particle size of (75–408 µm). Other parameters were kept constant while examining the effect of one parameter. Experiments were continued over pre-determined ranges of time until the dissolution rate of alumina got to a maximum. At the completion of the reaction, the slurry was filtered with a funnel and the residue washed using distilled water and dried at 60 °C for 24 h. The filtrate was diluted and analyzed for aluminum with the aid of an atomic absorption spectroscopy. The dealuminated residue was analyzed by SEM–EDS techniques [4, 5, 7, 8].

The dissolution of Owhe kaolinite in HNO_3 and H_2O_2 binary solution is represented by the equation below (Eq. 1).

$$2Al_2O_{3(s)} + 6HNO_{3(aq)} + H_2O_{2(aq)} \rightarrow 2Al(OH)_{3(aq)} + 2Al(NO_3)_{3(aq)} + H_2O_{(l)} + \frac{1}{2}O_{2(g)} \quad (1)$$

Results and discussion

Characterization

XRF analysis

The elemental analysis of the calcined kaolin by EDXRF technique revealed the major components of the clay as Mg (8.44%), Al (50.60%), Ti (5.43%), Si (24.58%), Fe (9.54%). Other minor and trace components of the clay include: P (0.22%), S

(0.48%), Ca (0.26%), Cr (0.06%), Mn (0.09%), Co (0.06%), Zn (0.03%), Ni (0.02%), and Ba (0.19%). The XRF result of Owhe kaolinite had earlier been reported [4].

XRD analysis

The minerals found in the kaolinite sample and their percentage distributions had earlier been reported. The radiation source used for the XRD was Cu (1.54 Å), generated at 45 kV and 40 mA. A fixed divergence slit was used with a divergence slit size of 1° and receiving slit size of 0.1 mm. Incident beam monochromator was not used for the analysis. The radius of the goniometer used was 240 mm while the temperature was set at 25 °C. The XRD result affirms the presence of kaolinite ($Al_2O_7{\cdot}SiO_2{\cdot}2H_2O$), muscovite $(KF)_2(Al_2O_3)_3(SiO_2)_6$, quartz ($SiO_2$), davyne ($Na_4K_2Ca_2Si_6Al_6O_{24}(SO_4)C_{l2}$), garnet ($Fe_3Al_2(SiO_4)_3$) and sanidine ($K(AlSi_3O_8)$), with principal peaks at 27.70, 26.85, 24.24, 21.15, and 20.16° 2θ [4].

Scanning electron micrograph (SEM) analysis

The morphology of the kaolinite particles was studied before leaching by scanning electron microscope (SEM). The result had been previously reported [4].

Effect of process variables

Effect of temperature of calcination on the leaching of alumina

The influence of temperature of calcinations on alumina leaching from Owhe kaolinite had earlier been reported [4]. Based on the result obtained, 750 °C was established as the best calcinations temperature.

Influence of H_2O_2 concentration in HNO_3 on Owhe kaolin dissolution

The effect of H_2O_2 concentration in a constant nitric acid concentration on Owhe kaolinite dissolution was investigated using H_2O_2 concentration range of 2–12 M over a range of 0–150 min at a constant HNO_3 concentration of 10 M. Other factors such as temperature, stirring rate, S/L ratio, and particle size were retained at 90 °C, 500 rpm, 15 g/L and < 75 µm. The plots on the effect of H_2O_2 concentration on the leaching of alumina from Owhe kaolinite is depicted in Fig. 1. The result reveals that the fraction of alumina leached rises with increase in H_2O_2 concentration over the time range studied [9]. Leaching rates of 58.2%, 66.9%, 78.3%, 82.4%, 87%, and 86.9% were attained with H_2O_2 concentrations of 2, 4, 6, 8, 10, and 12 M,. The result achieved with 12 M H_2O_2 (86.9 wt%) showed a small reduction compared to that achieved with 10 M H_2O_2 (87.0 wt%) within a time of 150 min, and this might be attributed to the obliteration of the configuration of the clay at higher concentration of the reagent. Thus, 10 M H_2O_2 in 10 M HNO_3 was engaged for other studies. With about 87.0 wt% alumina leaching within 150 min in 10 M H_2O_2/10 M HNO_3 binary solution, the leaching rate is higher, in comparison to when only HNO_3 was

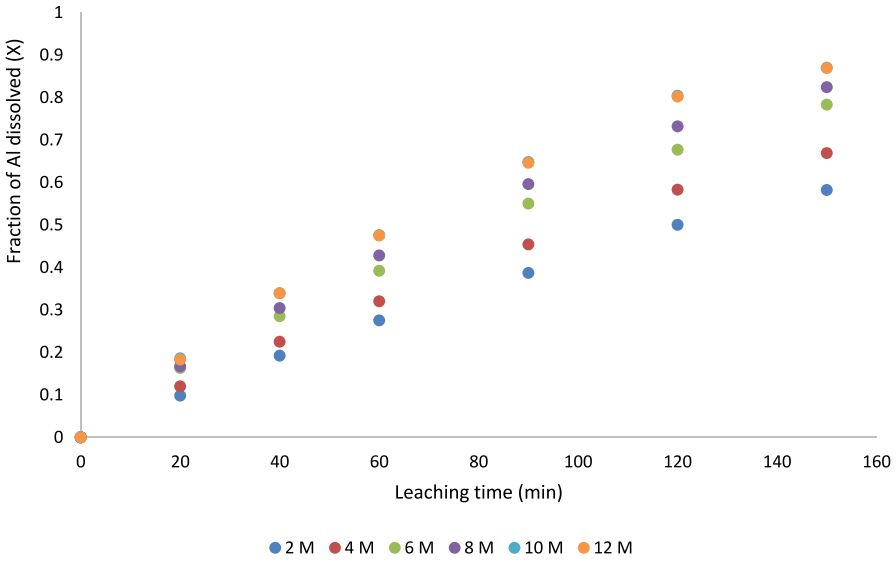

Fig. 1 Effect of H_2O_2 concentration in 10 M nitric acid on alumina leaching

used, where around 82.2 wt% was leached within the same time of contact [2]. This might be credited to the joint action of H_2O_2 and HNO_3. These agree with the results of previous researchers [4, 5, 7, 8].

Influence of temperature on the leaching of alumina

The influence of leaching temperature on the leaching of alumina from the kaolinite was examined with 40, 50, 60, 80, and 90 °C, while other experimental factors such as HNO_3 concentration, H_2O_2 concentration, S/L ratio, particle size and stirring rate were maintained at 10 M, 10 M, 15 g/L, < 75 µm and 550 rpm, correspondingly [10, 11]. The maximum dissolution rates of Owhe kaolinite at the temperatures above and the given experimental conditions were 57.1%, 67.0%, 80.2%, 87.7% and 89.6%. The leaching curves of alumina dissolution from Owhe kaolinite is shown in Fig. 2. The result reveals that temperature has a profound influence on the kaolinite rate of dissolution [12, 13]. The dissolution rate and the reaction speed increase as temperature increases [14]. This is attributed to the increase in the available energy occasioned by temperature increase for molecular and atomic collisions. The interface between the particles of kaolinite and the leachant raises the leaching rate.

About 89.6% alumina dissolution rate was recorded within 150 min at 90 °C with 10 M H_2O_2 in 10 M HNO_3. The value obtained from this study is higher by comparing it to leaching with only 10 M HNO_3 at similar dissolution conditions, which resulted to 85.2 wt% leaching rate. Therefore, higher dissolution obtained with 10 M HNO_3 in 10 M H_2O_2 might be ascribed to the joint effect of H_2O_2 and HNO_3. The result obtained here is similar to those of previous researchers [4, 5, 7, 8].

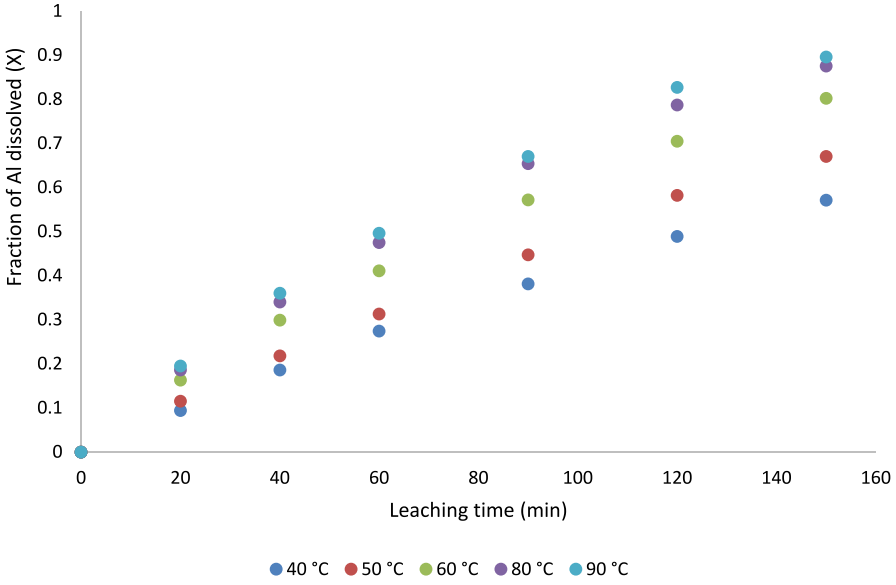

Fig. 2 Effect of temperature on alumina leaching

Influence of solid/liquid ratio on the leaching of alumina

The study on the influence of solid/liquid ratio on alumina leaching from Owhe kaolinite was investigated by testing solid/liquid ratios of 1.5/100, 2.2/100, 2.9/100, 3.6/100 and 4.3/100 g/mL. The values of H_2O_2 concentration, HNO_3 concentration, leaching temperature, stirring speed, and particle size were maintained constant at 10 M, 10 M, 90 °C, 550 rpm, < 75 µm over a time range of 0–150 min [15]. The leaching plots showing the fraction of alumina leached from the kaolinite within 150 min is depicted in Fig. 3. The highest leaching rates achieved within 150 min at the above S/L ratios and the given experimental conditions were 89.8%, 87.1%, 79.6%, 67.7% and 57.2%. The results show that the rate of leaching reduced when the S/L ratio was increased, signifying that S/L ratio increase has negative influence on the rate of leaching [12, 13, 16]. Previous works reported that increasing S/L ratio raises the quantity of solid in the reaction mixture, leading to a reduction in the leaching rate [4, 5, 17–19].

The results achieved in this work show a rise in the quantity of the alumina leached in comparison with 84.5% achieved when only HNO_3 was used as the leachant at the same experimental conditions [2]. This might be attributed to the joint action of H_2O_2 and HNO_3. This concurs with results obtained by Nnanwube et al. [4].

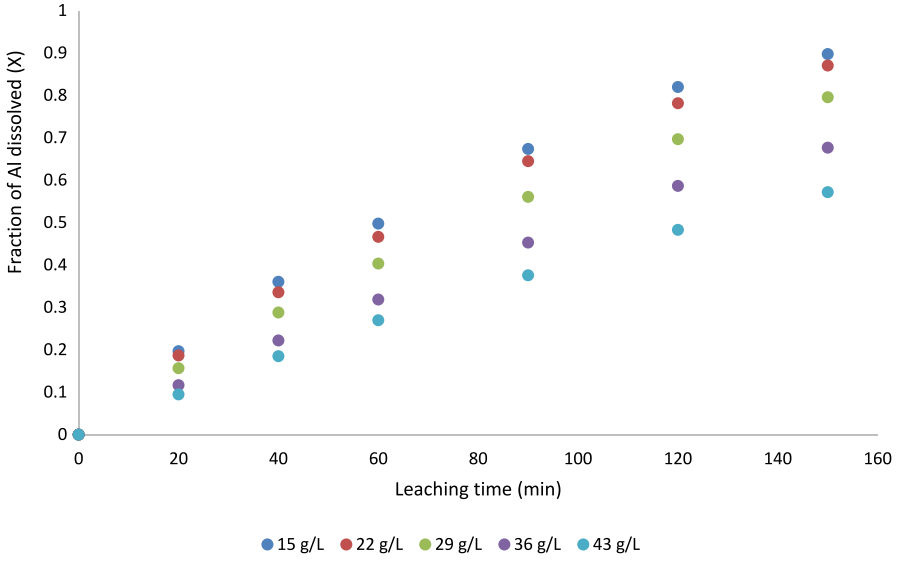

Fig. 3 Effect of solid/liquid ratio on alumina leaching

Influence of particle size on the leaching of alumina

The influence of particle size on alumina leaching from Owhe kaolinite was investigated using fractions of the sample with sizes of < 75, 75–106, 106–250,

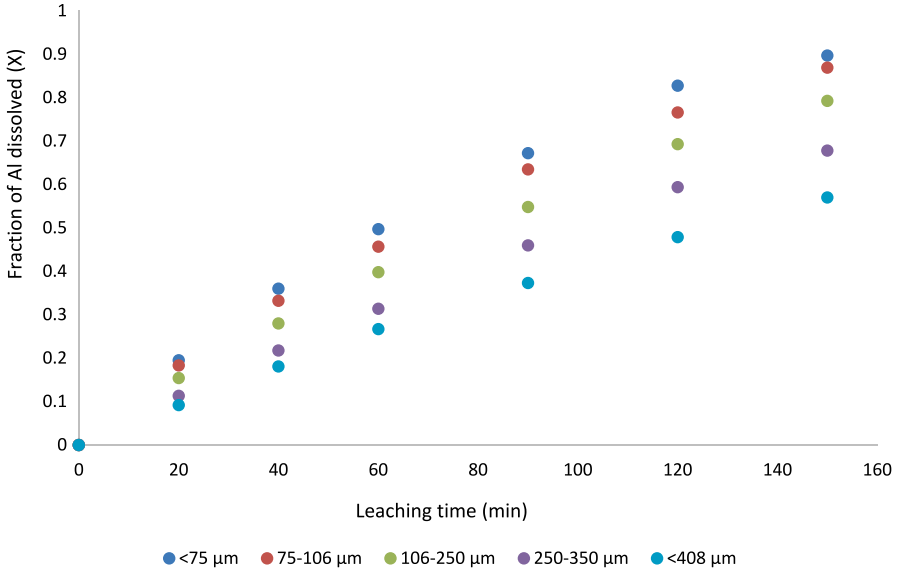

Fig. 4 Effect of particle size on the leaching of alumina

250–350, and < 408 µm, at fixed experimental conditions of 10 M H_2O_2 concentration, 10 M HNO_3 concentration, 550 rpm stirring speed, leaching temperature of 90 °C, and S/L ratio of 15 g/L over a range of time of 0–150 min [20]. The leaching plots showing the fraction of alumina leached at the particle sizes studied are shown in Fig. 4. Alumina fraction leached at the above particle sizes and the given experimental conditions were 0.897, 0.869, 0.793, 0.678 and 0.570, within 150 min. The result shows that, for a given duration, the leaching rate and speed of reaction increases as the kaolinite particle diameter reduces. The result also reveals a relative difference of 32.7% alumina leaching between the maximum and the minimum kaolinite particle size. Thus, higher particle sizes negatively influenced the leaching rate. This is ascribed to the rise in the surface area of the kaolinite particle as the size of the particle was decreased [12, 13]. With lesser particle sizes and a bigger surface area, more of the kaolinite is able to interact with the $O_2^{2-}$and NO_3^- ions in the solution, which increases the degree of kaolinite leaching [14].

About 89.7% of alumina was leached within 150 min at the experimental conditions in 10 M H_2O_2/10 M HNO_3 binary solution. The result reveals an increase in alumina leaching rate in comparison with 84.7 wt% obtained when HNO_3 was used alone at similar dissolution conditions [2]. This is ascribed to the combined effect of H_2O_2 and HNO_3. Similar result was reported by Nnanwube et al. [3].

Kinetic analysis

The kinetic investigation on the hydrometallurgical leaching of kaolinite used in this study in HNO_3/H_2O_2 binary solution was performed on the basis that the leaching system is a heterogeneous (liquid/solid) reaction system, requiring not only chemical reactions but mass transfer process. As proposed by the shrinking core models, the reaction rate for a liquid/solid system is typically controlled by one of the following: product layer diffusion, liquid film diffusion, and surface chemical reaction. For solid/fluid reaction system, Eq. 2 applies.

$$\mathrm{P(fluid)} + \mathrm{qQ(solid)} \quad \rightarrow \mathrm{Products} \tag{2}$$

Here P denotes the fluid used for the dissolution process, Q depicts the solid being leached and q represents the solid's stoichiometric coefficient. The slowest of the steps listed above is taken as the rate-determining step.

For a spherical particle, if the reaction rate is governed by the first step-diffusion through the fluid film, then the integral rate equation is constituted as follows [21] (Eq. 3).

$$\mathrm{X_B} = \frac{3\mathrm{b}k_g C_A}{\rho_B r_o t} = k_1 t \tag{3}$$

Here X_B is the fraction of B dissolved at time t; k_g the kinetic constant; b is the stoichiometric coefficient of the reagent in the leaching reaction; C_A the concentration of the leachants; ρ_B the solid material's density; r_o the original radius of the

solid material; t is the time of reaction; and k_1 is the rate constant. A plot of X_B versus t yields a slope equivalent to k_1. Hence, Eq. 4 applies.

$$\frac{dX_B}{dt} = k_1 \tag{4}$$

It has long been established that the correct way to examine how good hypothetical formulas concur with experiments is by fitting the measured pairs of values for the independent and dependent variables to the hypothetical formula using least squares method [22].

Assuming that there is a linear relationship (Eq. 5) between X_B and t, but the points do not lie on this straight line because of uncertainties in the measurements, then linear regression is a method of finding the most satisfactory straight line to represent the data.

$$X_B = X_B(t) = I + k_1\ t; \text{where } I = X_B(0) \text{ and } k_1 = \frac{dX_B}{dt} \tag{5}$$

The problem involves estimating the most appropriate values of I and k_1 that, on the basis of their graphical interpretation, are generally known as the intercept and slope of the required relationship [23].

By applying least squares method to Eq. 5, I and k_1 can be estimated. The standard error of estimate ($S_{X_B.t}$) and the coefficient of correlation (R^2) can also be estimated using standard methods.

From the experimental data depicted in Figs. 1, 2, 3, and 4, k1, $S_{X_B.t}$, and R^2, were estimated for the various values of the H_2O_2 concentration, temperature, S/L ratio, and particle diameter, as shown in Table 1.

By varying the temperature while maintaining other parameters constant, the activation energy of the process is estimated using Eq. 6 [24].

$$k = Ae^{\frac{E_a}{RT}} \tag{6}$$

Here k designates the reaction rate constant; E_a designates the apparent activation energy; A designates the frequency factor; T and R are temperature and gas constant.

By the linearization of Eqs. 6, 7 is obtained [25–27].

$$\text{Ln } k = \text{Ln } A - \frac{E_a}{RT} \tag{7}$$

From the plot of Ln k versus 1/T, the activation energy, E_a, is obtained. The plot was analyzed using least squares method and activation energy of 4406 J mol^{-1} was obtained. The frequency factor was also calculated to be 0.023 s^{-1}.

The activation energy (E_a) obtained in this study is lower than the values obtained by other authors as depicted in Table 2. This may be attributed to the least squares method used in estimating the rate constant values at various temperatures. It has been posited that E_a less than 20 kJ mol^{-1} implies that a system is diffusion controlled [24]. It has

Table 1 Apparent rate constant (k_1) ± standard error ($S_{X_B \cdot t}$), and correlation coefficient (R^2) of the variables studied

H_2O_2 concentration (M)	2	4	6	8	10	12
Apparent rate constant (k_1) (min^{-1}) ± standard error ($S_{X_B \cdot t}$)	$3.734 \times 10^{-3} \pm 0.0158$	$4.27 \times 10^{-3} \pm 0.0203$	$4.78 \times 10^{-3} \pm 0.0243$	$5.10 \times 10^{-3} \pm 0.0359$	$5.35 \times 10^{-3} \pm 0.0485$	$5.35 \times 10^{-3} \pm 0.0486$
Correlation coefficient (R^2)	0.9936	0.9928	0.9916	0.9843	0.9736	0.9740
Leaching temperature (°C)	40	50	60	80	90	
Apparent rate constant (k_1) ± standard error ($S_{X_B \cdot t}$)	$3.67 \times 10^{-3} \pm 0.0168$	$4.33 \times 10^{-3} \pm 0.0187$	$4.93 \times 10^{-3} \pm 0.0310$	$5.33 \times 10^{-3} \pm 0.0457$	$5.45 \times 10^{-3} \pm 0.0504$	
Correlation coefficient (R^2)	0.9934	0.9936	0.9872	0.9763	0.9726	
Solid/Liquid ratio (g/L)	15	22	29	36	43	
Apparent rate constant (k_1) ± standard error ($S_{X_B \cdot t}$)	$5.42 \times 10^{-3} \pm 0.0494$	$5.30 \times 10^{-3} \pm 0.0424$	$4.93 \times 10^{-3} \pm 0.0293$	$4.35 \times 10^{-3} \pm 0.0190$	$3.66 \times 10^{-3} \pm 0.0137$	
Correlation coefficient (R^2)	0.9736	0.9795	0.9884	0.9940	0.9950	
Particle size (μm)	75	106	250	350	408	
Apparent rate constant (k_1) ± standard error ($S_{X_B \cdot t}$)	$5.46 \times 10^{-3} \pm 0.0509$	$5.28 \times 10^{-3} \pm 0.0380$	$4.94 \times 10^{-3} \pm 0.0264$	$4.43 \times 10^{-3} \pm 0.0221$	$3.66 \times 10^{-3} \pm 0.0133$	
Correlation coefficient (R^2)	0.9724	0.9833	0.9908	0.9918	0.9952	

Table 2 Values of activation energy estimated from other studies

Clay type	Leachant	Activation energy (E_a) (kJ/mol)	Mechanism	References
Kaolinite	Hydrochloric acid	34.0	Liquid film diffusion	Udeigwe et al. [28]
Kaolinite	Hydrochloric acid and Hydrogen peroxide	53.92	Diffusion control	Nnanwube et al. [4]
Kaolinite	Nitric acid and Hydrogen peroxide	26.56	Chemical reaction	Nnanwube and Onukwuli [7]
Kaolinite	Nitric acid	26.40	Chemical reaction	Nnanwube and Onukwuli [8]
Kaolinite	Nitric acid and Hydrogen peroxide	4.41	Chemical reaction	This study

also been posited that in most cases, the rate-controlling step of the mixed leaching system is better obtained from plots of kinetic equations instead of the E_a [7, 8].

As posited by the SCM, the kinetics of a diffusion-controlled process is proportionate to the inverse of the square of the initial particle radius (r_o), while for a process governed by chemical reaction, k is proportionate with the reciprocal of the initial particle radius [28]. By using least squares analysis, a more linear relationship is observed by plotting k versus ($1/r_o$) ($R^2 = 0.7384$), compared to the plot of k versus ($1/r_o)^2$ ($R^2 = 0.6400$) confirming that the leaching process is chemical reaction controlled [7, 8, 29].

A model that relates the effects of process variables and the rate constant of the leaching reaction is proposed as shown in Eq. 8 [8].

$$k_1 = k_o(LC)^e(PD)^f(SL)^g e^{-\frac{E_a}{RT}} \tag{8}$$

Substituting Eq. 3 into Eq. 8 gives Eq. 9.

$$X_B = k_o(LC)^e(PD)^f(SL)^g e^{-\frac{E_a}{RT}}\, t \tag{9}$$

LC, PD, SL, E_a, R, and T denote the leachant concentration, particle diameter, and solid/liquid ratio, activation energy, ideal gas constant, and temperature. The constants e, f, and g are the reaction orders with respect to the various parameters shown in Eq. 8 [12, 13, 15].

If the leachant concentration is varied while other variables are kept constant, Eq. 9 changes to Eq. 10.

$$X_B = k_o(LC)^e t \tag{10}$$

Differentiation of Eq. 10 gives Eq. 11.

$$d[X_B]/dt = k_o(LC)^e \tag{11}$$

$d[X_B]/dt$ represent the slope when X_B is plotted against t for different leachant concentrations depicted in Fig. 1. The constant 'e' is found from the slope of Ln [$d[X_B]/dt$] against Ln (LC) [13]. Likewise, f and g were found from the plots of Ln [$d[X_B]/dt$] versus Ln (PD), and Ln [$d[X_B]/dt$] versus Ln (SL). From least squares analysis of the plots, the constants were obtained as $e = 0.215 \pm 0.0185$, $f = -1.706 \pm 0.1867$, and $g = -0.352 \pm 0.0812$. By substitution of the reaction orders at the optimal conditions of the various parameters, activation energy, gas constant, and the average recovery fraction of alumina, (0.890), into Eq. 9, the rate constant of the leaching process was obtained as 1.067 s^{-1}. Hence the kinetic expression for the leaching process is obtained as Eq. 12.

$$X_B = 1.067(LC)^{0.215}(PD)^{-1.706}(SL)^{-0.352} e^{-\left(\frac{4406}{RT}\right)} t \tag{12}$$

a. SEM image of Owhe kaolinite leached with 10 M H_2O_2/10 M HNO_3

Fig. 5 SEM image of Owhe kaolinite leached with 10 M H_2O_2/10 M HNO_3

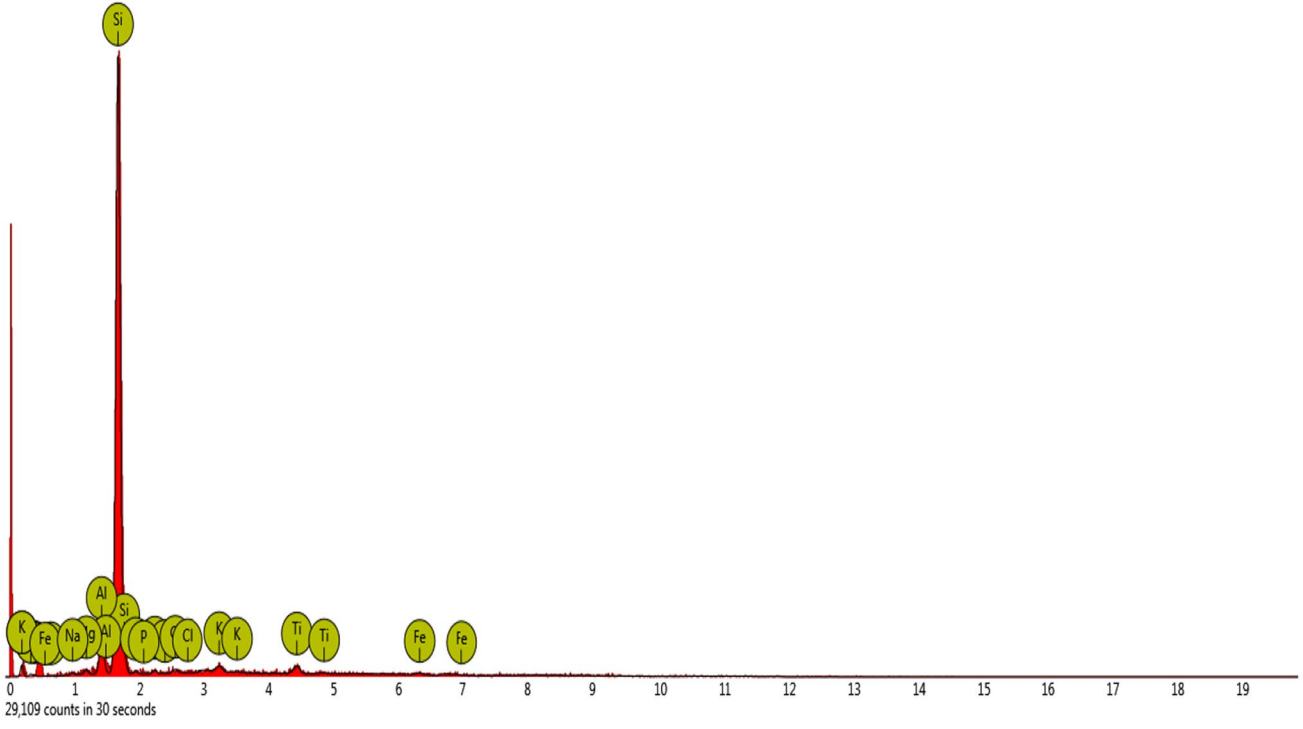

b. EDS of Owhe kaolinite leached with 10 M H_2O_2/10 M HNO_3.

Fig. 6 EDS of Owhe kaolinite leached with 10 M H_2O_2/10 M HNO_3

Post-leaching analysis

SEM–EDS analysis of Owhe kaolinite clay after leaching with 10 M H_2O_2/10 M HNO_3

The morphology and elemental composition of Owhe kaolinite leached with 10 M H_2O_2/10 M HNO_3 was examined by SEM (Fig. 5) joined with EDS and shown in Fig. 6. The micrograph of the residues reveals an increase in the solid's roughness due to reaction with the lixiviant [30]. The EDS (Fig. 6) of the residue revealed that Si (82.38 wt%), Al (5.30 wt%), Ti (4.53 wt%), K (1.77 wt%), P (1.00 wt%), S (1.14 wt%), Cl (0.92 wt%), Fe (2.13 wt%), Mg (0.55 wt%), and Na (0.27 wt%), were present in the clay.

Conclusions

The feasibility of HNO_3 and H_2O_2 solution as lixiviant for the leaching of alumina from kaolinite obtained from Owhe was investigated in this study. The result of XRD analysis showed the minerals found in the clay as kaolinite, muscovite, quartz, davyne, garnet, and sanidine, while elemental analysis showed the presence of 50.0 wt% aluminum, 24.58 wt% silicon, 9.54 wt% iron, and 8.44 wt% magnesium, 5.43 wt% titanium, as main elements. Zn, Ni, Co, Mn, Cr, Ca, S, P and Ba, however, occurred as minor and trace elements. The experimental data were found to fit into the chemical reaction model, which was also the rate-determining step with activation energy of 4.406 kJ/mol. About 89% alumina was recovered from an initial 15 g/L after about 150 min of reaction at the optimal conditions. Hence, least squares method was adequate to evaluate the kinetic data.

Funding This research received no funding.

Declarations

Conflict of interest This research has no conflict of interest.

References

1. Nnanwube IA, Keke M, Onukwuli OD (2024) Kinetics of Owhe kaolinite leaching for alumina recovery in hydrochloric acid solution. Sci Afr 23:e02045. https://doi.org/10.1016/j.sciaf.2023.e02045
2. Nnanwube IA, Keke M, Onukwuli OD (2024) Assessment of calcined Owhe kaolinite for potential alumina recovery via nitric acid route. Results Chem 7:101262. https://doi.org/10.1016/j.rechem.2023.101262
3. Nnanwube IA, Onukwuli OD, Ekumankama EO (2022) Assessment of Amagunze microcline for alumina recovery in nitric acid and hydrogen peroxide solutions and kinetic study. Can Metall Q 62(2):330–344. https://doi.org/10.1080/00084433.2022.2099725

4. Nnanwube IA, Keke M, Onukwuli OD (2022) Assessment of Owhe kaolinite as potential aluminium source in hydrochloric acid and hydrogen peroxide solutions: kinetics modeling and optimization. Clean Chem Eng 2:100022. https://doi.org/10.1016/j.clce.2022.100022
5. Siddique NA, Kurny ASW (2010) Kinetics of leaching alumina from discarded high alumina refractory bricks. Int J Eng Technol 10(1):19–22
6. Nnanwube IA, Onukwuli OD (2020) Modeling and optimization of zinc recovery from Enyigba sphalerite in a binary solution of hydrochloric acid and hydrogen peroxide. J Southern Afr Inst Mining Metall 120(11):609–616
7. Nnanwube IA, Onukwuli OD (2022) Oxidative leaching of Akpugo kaolinite for alumina recovery and kinetic modeling. J Sustain Metall 8(4):1727–1743. https://doi.org/10.1007/s40831-022-00603-y
8. Nnanwube IA, Onukwuli OD (2023) Characterization and kinetics of alumina leaching from calcined Akpugo kaolinite for potential aluminum recovery. S Afr J Chem Eng 43:24–37
9. Nnanwube IA, Onukwuli OD (2018) Kinetics and mechanisms of nitric acid leaching of alumina from Amagunze clay. J Eng Appl Sci 13:63–82
10. Wu Z, Dreisinger DB, Urch H, Fassbender S (2014) The kinetics of leaching galena concentrates with ferric methanesulfonate solution. Hydrometallurgy 142:121–130. https://doi.org/10.1016/j.hydromet.2013.10.017
11. Tanaydin MK, Demirkiran N (2018) Investigation of selective leaching and kinetics of copper from malachite ore in aqueous perchloric acid solutions. Sep Sci Technol 54(5):1–13. https://doi.org/10.1080/01496395.2018.1512619
12. Kocan F, Hicsonmez U (2019) Leaching of celestite in sodium hydroxide solutions and kinetic modeling. J Dispers Sci Technol 40(1):43–54. https://doi.org/10.1080/01932691.2018.1464466
13. Kocan F, Hicsonmez U (2019) Leaching kinetics of celestite in nitric acid solutions. Int J Miner Metall Mater 26(1):11–20. https://doi.org/10.1007/s12613-019-1705-0
14. Ma J, Tang Y, Yang DQ, Pei P (2020) Kinetics of advanced oxidative leaching of pyrite in a potassium peroxydisulphate solution. J South Afr Inst Mining Metall 120:165–172
15. Tanaydin MK, Tanaydin ZB, Demirkiran N (2021) Determination of optimum process conditions by central composite design method and examination of leaching kinetics of smithsonite ore using nitric acid solution. J Sustain Metall 7:178–191. https://doi.org/10.1007/s40831-020-00333-2
16. Bayrak B, Lacin O, Sarac H (2010) Kinetic study on the leaching of calcined magnesite in gluconic acid solutions. J Ind Eng Chem 16(3):479–484. https://doi.org/10.1016/j.jiec.2010.01.055
17. Kunkul A, Gulezgin A, Demirkiran N (2013) Investigation of the use of ammonium acetate as an alternative lixiviant in the leaching of malachite ore. Chem Ind Chem Eng Quart 19(1):25–35. https://doi.org/10.2298/CICEQ120113033K
18. Nnanwube I, Udeaja J, Onukwuli O (2020) Kinetics of zinc recovery from Enyigba sphalerite in a binary solution of acetic acid and sodium nitrate. Aust J Basic Appl Sci 14(5):1–11
19. Nnanwube IA, Udeaja JN, Onukwuli OD (2020) Kinetics of zinc recovery from sphalerite in acetic acid solution. J Mater Environ Sci 11(3):499–511
20. Sakultung S, Pruksathorn K, Hunsom M (2008) Simultaneous recovery of Ni and Co from scrap mobile phone battery by acid leaching process. Asia-Pac J Chem Eng 3(4):374–379. https://doi.org/10.1002/apj.158
21. Levenspiel O (1999) Chemical reaction engineering, 3rd edn. Wiley, New York
22. Lente G (2018) Facts and alternative facts in chemical kinetics: remarks about the kinetic use of activities, termolecular processes, and linearization techniques. Curr Opin Chem Eng 21:76–83. https://doi.org/10.1016/j.coche.2018.03.007
23. Mashkina E, Oldham KB (2015) Linear regressions to which the standard formulas do not apply. Chem Texts 1:11
24. Qu B, Deng L, Deng B, He K, Liao B, Su S (2018) Oxidation Kinetics of dithionate compound in the leaching process of manganese dioxide with manganese dithionate. React Kinet Mech Catal 123:743–745. https://doi.org/10.1007/s11144-017-1284-x
25. Yang S, Li H, Sun Y, Chen Y, Tang C, He J (2016) Leaching kinetics of zinc silicate in ammonium chloride solution. Trans Nonferr Metals Soc China 26(6):1688–1695. https://doi.org/10.1016/S1003-6326(16)64278-4
26. Moyo LB, Simate GS, Mamvura TA (2022) Maghnesium recovery from ferrochrome slag: kinetics and possible use in a circular economy. Heliyon 8:e12176. https://doi.org/10.1016/j.heliyon.2022.e12176

27. Nikolic I, Drincic A, Djurovic D, Karanovic L, Radmilovic VV, Radmilovic VR (2016) Kinetics of electric arc furnace slag leaching in alkaline solutions. Constr Build Mater 108:1–9. https://doi.org/10.1016/j.conbuildmat.2016.01.038
28. Udeigwe U, Onukwuli OD, Ajemba R, Ude CN (2015) Kinetics studies of hydrochloric acid leaching of aluminium from Agbaja clay. Int J Res Adv Eng Technol 1(1):64–72
29. Souza AD, Pina PS, Leao VA (2007) Bioleaching and chemical leaching as an integrated process in the zinc industry. Miner Eng 20(6):591–599. https://doi.org/10.1016/B978-0-12-804022-5.00001-3
30. He S, Wang J, Yan J (2011) Pressure leaching of synthetic zinc silicate in sulfuric acid medium. Hydrometallurgy 108(3–4):171–176. https://doi.org/10.1016/j.hydromet.2011.04.004

Publisher's Note Springer Nature remains neutral with regard to jurisdictional claims in published maps and institutional affiliations.

Springer Nature or its licensor (e.g. a society or other partner) holds exclusive rights to this article under a publishing agreement with the author(s) or other rightsholder(s); author self-archiving of the accepted manuscript version of this article is solely governed by the terms of such publishing agreement and applicable law.